2024 IEEE/RSJ International Conference on Intelligent Robots and Systems (IROS)
October 14-18, 2024. Abu Dhabi, UAE

Design of a Soft Shell for a Spherical Exploration Robot Traversing Varying Terrain

Meghali Prashant Dravid, Micah Oevermann, David McDougall, David Dugas, and Robert Ambrose(*IEEE Member*)

***Abstract*— Exploration robots are typically equipped with either wheels or legs for mobility. However, these conventional designs inherently possess certain limitations, such as restricted ability to navigate through steep slopes, soft soil or muddy watery terrain. Despite the advancements in robotics technoloy, these challenges persist in both terrestrial and extraterrestrial environments. To overcome these obstacles, we have proposed a novel solution in the form of a spherical robot with a soft shell. This paper provides an overview of the construction of this spherical robot and the design of its soft shell for adapting to varying terrain. Furthermore, we analyze and characterize its performance across various terrain types as the shell pressure is changed. By employing this approach, the paper establishes the suitability and efficiency of the spherical robot in traversing different terrain by adapting the shell pressure.**

I. INTRODUCTION

Whether it is NASA's Artemis program, agriculture, construction or a military endeavor, the deployment of robots across difficult terrain has garnered significant interest and has intensified efforts in creating mobility platforms.

The Lunar landscape lacks any natural weathering process to erode or smooth out its soil. As a result, it is by nature rough and the impact-generated dust is highly abrasive [1]. Any wheeled or tracked rover on the lunar surface must be adequately protected from this drive-train-destroying dust. Traditional wheeled rover systems use protective dust jacket over mechanisms, and use seals at every joint. Depending on the complexity of the rover, the fine particles may still find a way in [2].

Spherical-shaped rovers offer a geometrically refreshing take on the extraterrestrial mobility problem. These types of robots have shown promise as niche extraterrestrial explorers [3]. Their geometrical advantage allows them to tumble across rough terrain as shown by JPL's Tumbleweed rover [4]. Their spherical shape makes them ideal for rolling down steep slopes or into craters. All they need is gravity. When a pendulum or flywheel is added, it can be used to actively explore various surfaces, even in water [5], [6]. As an added benefit, all important communications, sensing, and motion systems are enclosed within its shell, protecting them from impacts and disastrous effects of lunar dust particles. However, most spherical robots that have been constructed use rigid outer plastic shells. This ignores any potential dynamic benefit of a soft pressurized outer shell [7].

**Research supported by the Texas A&M Chancellor's Research Initiative and matching funds from the Texas Governor's University Research Initiative.

Authors are with Texas A&M University, College Station TX, 77843 USA R.O Ambrose's e-mail is rambrose@tamu.edu

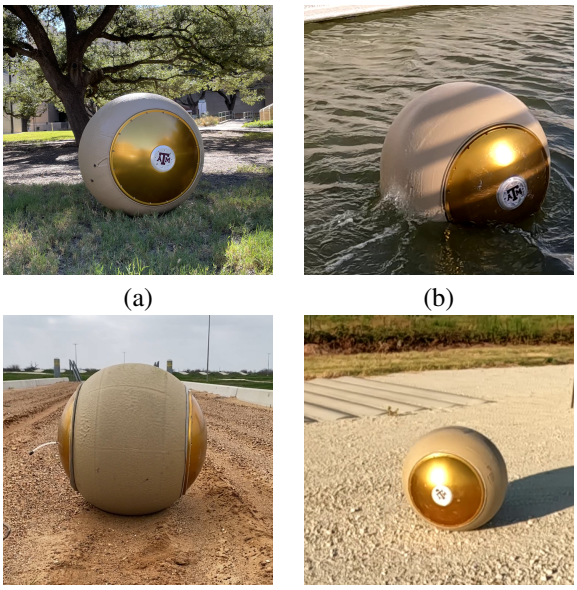

Fig. 1. RoboBall in various terrain: (a) Rolling on grass (b) Rolling through water (c) Traversing on sand (d) Rolling over gravel

Accurately characterizing wheel-soil interactions is crucial for predicting rover locomotion performance throughout the various phases of a planetary robotic mission, including design, validation, and operational stages. This capability is essential for ensuring the success and effectiveness of such missions. The evaluation of driving performance of the robot has long relied on the tractive effort the engine can produce at the wheels and the power consumption or fuel efficiency of the vehicle. Particularly in soft extraterrestrial soils, reducing ground pressure enhances a robot's mobility—a critical consideration for planetary robotic missions. Limited efforts have explored extending these techniques to spherical systems with single point of contact.

We propose a novel spherical robot, with a dynamic, soft, pressurized outer shell. The robot is driven by an internal 2 - DOF pendulum and has an internal pneumatic system. The system is capable of actively servoing while adapting its ground pressure to explore and traverse a variety of terrain [8]. With such a system it would be valuable to characterize its thrust and predict its ability to navigate on various terrain. This paper emphasizes design criteria for the soft shell and the characteristics of the shell in terms of robot performance on different terrain types.

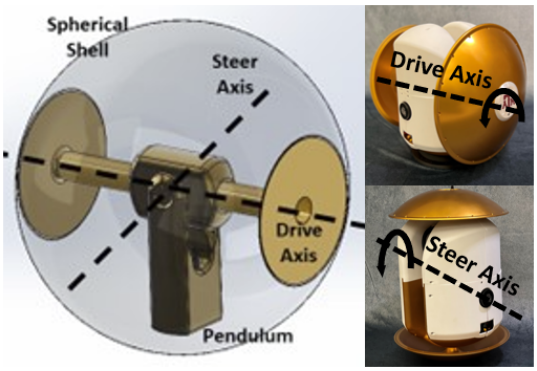

Fig. 2. Pendulum and hubs assembly. Deployed (left upper), and folded (left lower)

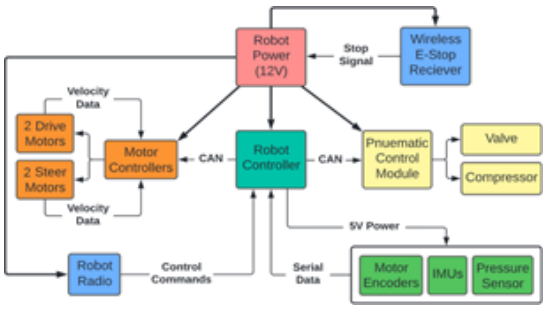

Fig. 3. Diagram of roboBall's internal control architecture

II. Robot Architecture

The robotic system, named "RoboBall", consists of an inner 2- DOF pendulum rigidly connected to the outer shell through an axel and aluminum hubs. The pendulum is designed such that there is a 2 inch gap between it and the 24 inch diameter shell. An overview of the robotic pendulum is shown in Figure 2 with the 2 motion axes illustrated, but with the outer shell removed. The pendulum is equipped with two sets of BLDC (Brush-less Direct Current) motors to actuate these drive and steer axes. This will raise the pendulum and change RoboBall's center of gravity allowing the system to roll or steer.

At a high level, the robot's control architecture consists of the robot's internal computer with the motor controllers, sensing array, and internal pneumatic system. The motor controllers communicate with the central RoboRio computer over CAN protocol. System IMUs, pressure sensors, and encoders are connected over serial with USB connections. The robot is designed with an internal pneumatic system to control the shell pressure. Commands are fed in through a joystick from a host computer to the robot's radio. Figure 3 represents a schematic between the connections of these systems.

The internal pneumatic system is equipped with a small compressor and tank system to vary its internal pressure in situ, shown in figure 4. To operate, the robot will start with its tanks half full. To decrease its internal pressure the robot will use its internal compressor to move air from the ball into the tanks. When the valve is opened and tanks are vented, air

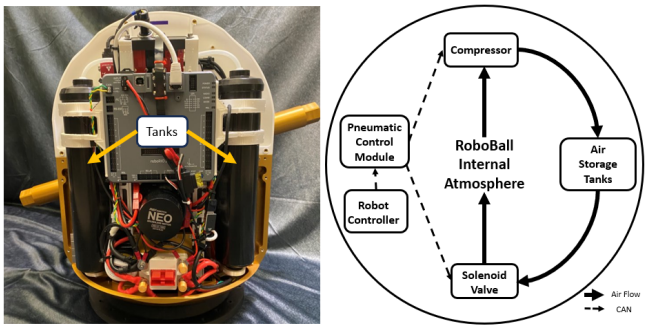

Fig. 4. Diagram of roboBall's internal pneumatic system

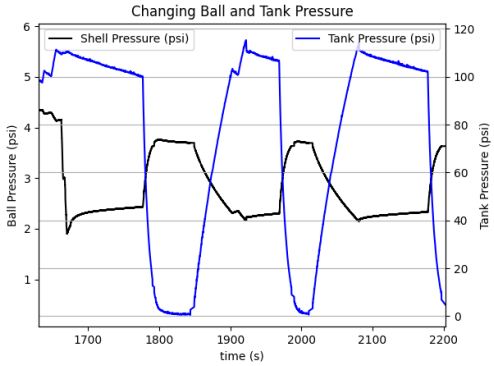

Fig. 5. This figure illustrates the effect of moving air between tank and shell to inflate or deflate the system

is released from the tanks to pressurize the shell. This change is monitored with pressure sensors within the tanks and on the pendulum. Varying ball pressure is shown in figure 5.

The pendulum can steer in one direction 90 degrees, enabling the robot to be removable from the shell holes for ease of maintenance, troubleshooting, and charging. Initially, a system of two rings permanently clamped on the interior yoga ball to serve as pneumatic bladder. The ball within the rings was flexible enough to provide an airtight seal, an o-ring and sealing screws provide the final seal to attach the hubs to the rings. A section view of the assembly is shown in figure 6. Due to lack of rigidity for environmental testing in the first shell a molded shell is adopted for this study. A detailed explanation of this shell construction can be found in the [9]. The robot can then be folded as in figure 2 and dropped into the shell.

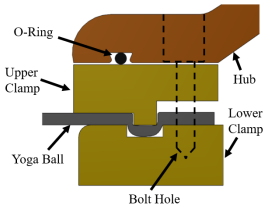

Fig. 6. Interface from soft shell to rigid hubs

III. Design of Soft Shell

This section outlines the methodology and criteria limitations employed in designing the soft pneumatic shell for the robot.

A. Design Criteria

In the development of a soft spherical outer shell with adjustable pressure capabilities, we must adhere to two critical design requirements. Firstly, the shell must possess the strength to withstand a minimum operating pressure without losing its shape. This ensures the stability and integrity of the robot's spherical form. Secondly, it must maintain this spherical geometry consistently, even under pressure, to allow for unrestricted movement of the pendulum while preserving the robot's symmetrical structure. These design considerations are paramount for achieving optimal performance and functionality of the robot in various applications.

1) Operating Static Pressure: When a soft body is placed on a hard surface, it will deform to that surface in a way that is related to its pressure. A schematic of this effect in shown in Figure 7. Where W_b is the total system weight, P is the internal shell pressure, R is the nominal outer radius (12in in this case), d_{flat} is the diameter of the flat section, and δ is the amount deflected from nominal radius. W_b, d_{flat}, and P are related through (1). This arises through assuming the area of the flat is a circle and related to the static weight with the force of the internal pressure over the flat area.

$$d_{flat} = \sqrt{\frac{4W_b}{\pi * P}} \tag{1}$$

This model was experimentally validated in our previous work [8] where we found our nominal operating pressure to be between 3-5psi. We can apply a simple transformation to determine our robot's ground pressure, and vital when modeling traction.

$$P_{ground} = \frac{W_b}{A_{flat}} = \frac{4W_b}{\pi d_{flat}^2} \tag{2}$$

Which is synonymous with the systems internal pressure.

2) Sphericality: When soft objects are inflated they tend to expand. Excessive expansion of a sphere with one axis rigidly held will turn it into an ellipse and turn a rolling problem into a balancing problem. As such, we desire to create a shell that will maintain its spherical shape at our operating pressure. To quantify this parameter, we measured the outer diameter of the inflated shell (shown in Figure 8(d))and normalized it with the ideal outer radius of the shell. This is shown in (3) where $R_{expanded}$ is measured, R_{ideal} is 12in, and b is defined as a unitless shape parameter. When $b < 1$ the system is underinflated, $b = 1$ indicates the system is at the desired shape, and when $b > 1$ the system is overinflated.

$$b = \frac{R_{expanded}}{R_{ideal}} \tag{3}$$

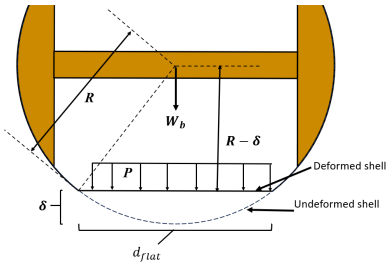

Fig. 7. Schematic of a soft spherical shell deforming on a flat surface

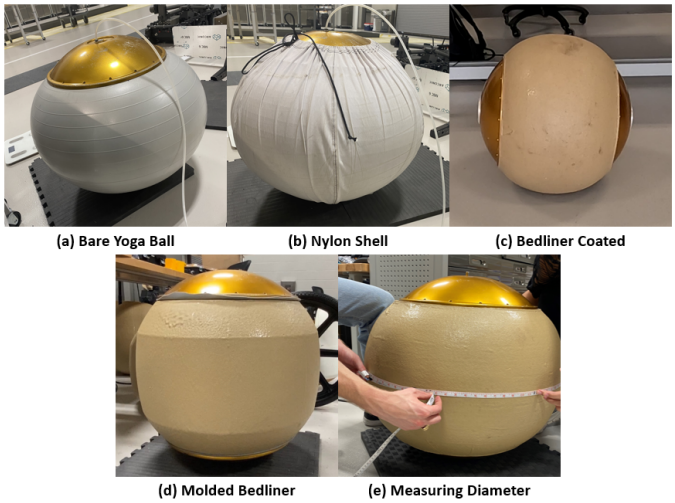

Fig. 8. Pictures of all prototypes

B. Construction and Fabrication

In our design of the outer shell, we considered four prototypes. Three variations use a yoga ball clamped between two permanent rings as a base and for the forth a 3D printed mold is uses as a base. The first prototype was a bare unconstrained yoga ball, the second used a sewn nylon jacket to constrain the ball, for the third, we swapped the nylon jacket for a flexible elastomer that was sprayed on, and the forth the yoga ball was replaced by a 3D printed internal mold on which the elastomer was sprayed. The third and the forth prototypes are close to the system's final shape. All are shown in Figure 8.

C. Shell Prototype Variations

Three different variations of shell were tested. One with a bare yoga ball as a control, a second with a sewn nylon jacket constraint, and a final one with a sprayed-on elastomer bedliner.

Each of the prototype shells was tested against our design parameters. As they were inflated we measured the outer diameter of the shell as demonstrated in Figure 8(e). We terminated the experiment when the shell either burst or reached the edge of our operating pressure range. The results are shown in Figure 9. Of all four prototypes, both the elastomer-coated shells were able to reach our desired pressure with minimal deviation in spherical shape, however

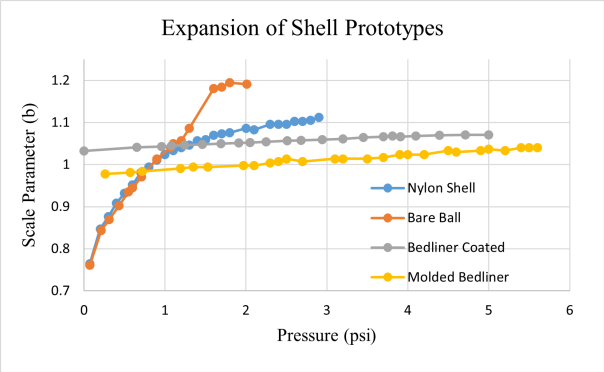

Fig. 9. Shell expansion results at variable pressures, reproduced from [9]

due to the ease in reproducibility, molded bedliner shell was chosen for our terrain experiments.

IV. Dynamical Behaviour

The earlier section discussed the design criteria based on the static behavior of the shell. In order to gain insight into the dynamic behavior of the shell, we focused on two key parameters: tractive effort and power consumption. These choices were influenced by extensive research conducted on vehicles, which aimed to understand how they perform under different speeds and gear ratios. Figure 10 shows tractive effort vs. vehicle speed characteristic curve for a common tire. This is an ideal assumption with 100% engine efficiency, This curve can be utilized to optimize the engine power consumption. By drawing parallels with this research on tires, we identified tractive effort and power consumption as crucial metrics for comprehending the operational behavior applied to a spherical, soft robot.

In this section, we present our set up and results for multiple experiments conducted to show characteristics of the proposed soft shells. This section also provides a comparative analysis of the robot's performance across two subsections. Firstly, it examines the impact of varying terrain on the robot's performance. Secondly, it investigates how different shell thicknesses affect the robot's behavior. Additionally, it evaluates the robot's performance in water, as an extreme

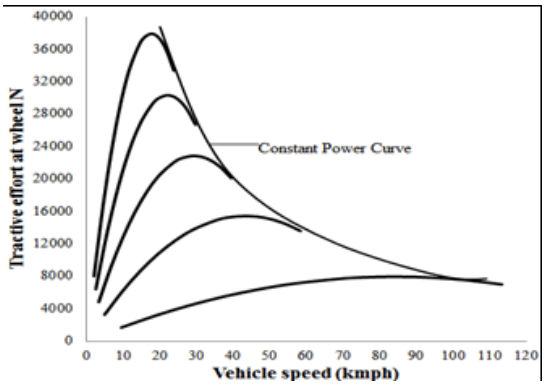

Fig. 10. Ideal tractive effort curve [10]

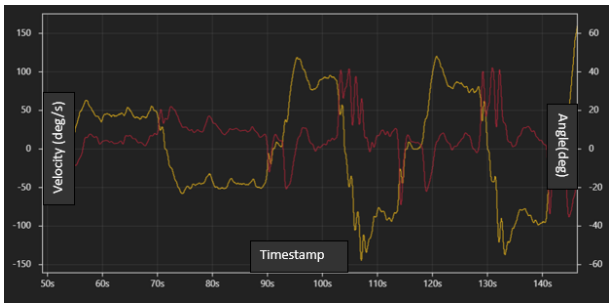

Fig. 11. Raw data for drive velocity and drive angle

terrain case, offering a comprehensive understanding of its capabilities across different environments.

A. Terrain Variation

The effectiveness of robotic systems across different terrain relies heavily on how well they manage tractive effort and power consumption. Accurate measurement and understanding of these parameters are essential for optimizing robot design and operation. To this end, we equip our robot with a suite of sensors, including motor encoders, IMUs, and pressure sensors, enabling comprehensive data collection during experimental trials. These sensors allow us to gather detailed data during our experiments. Our research looks into how different terrains affect the robot. By conducting multiple trials at different pressure levels, we're aiming to uncover how these terrains impact tractive effort and power usage. Our goal is to deepen our understanding of how robots interact with different surfaces, which can ultimately help us design and operate them more effectively. In our experiments, we make sure to keep things consistent by driving the robot in a controlled environment along a straight path. This helps us gather data in a uniform manner across all our trials. We are conducting experiments for different pressures ranging from 1 PSI to 5 PSI. At each pressure we run the experiment twice to make sure our results are reliable and consistent. Our focus is on two types of terrain: concrete and sand, which are commonly encountered in real-life scenarios. Figure 11 illustrates the raw measurements of angular drive velocity in (deg/s) and drive angle in degrees. Yellow line represents the drive velocity and red represents the drive angle in figure 11.

From the drive angle and drive velocity we can then calculate the torque (T), power (P) and tractive effort (TE) as follow, The Robot parameters are:

- Mass of the Robot, M = 40 kg
- Gravitational acceleration, g = 9.81 m/s
- Effective Length of the Pendulum l = 0.0975 m
- Radius of the Shell, R = 0.3048 m
- Drive Gear Reduction, G = 1:21

$$T = Mglsin(\theta) \tag{4}$$

$$P = T\omega \tag{5}$$

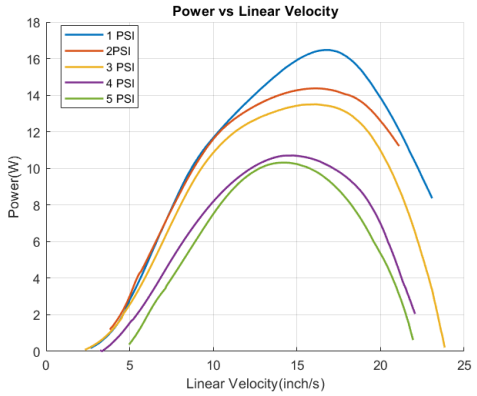

(a) Power vs Linear Velocity

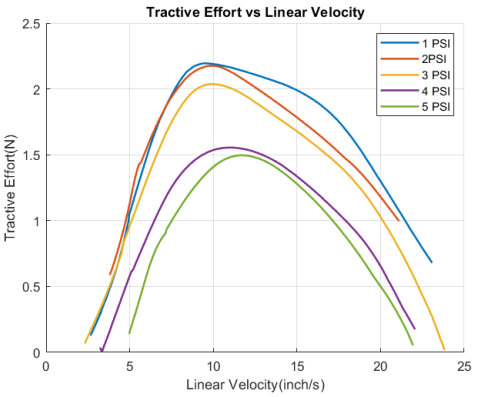

(b) Tractive Effort vs Linear Velocity

Fig. 12. RoboBall on concrete

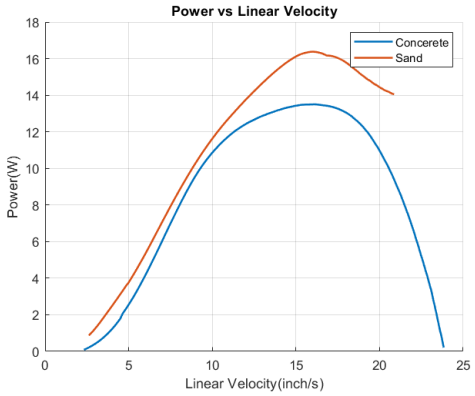

(a) Power vs Linear Velocity

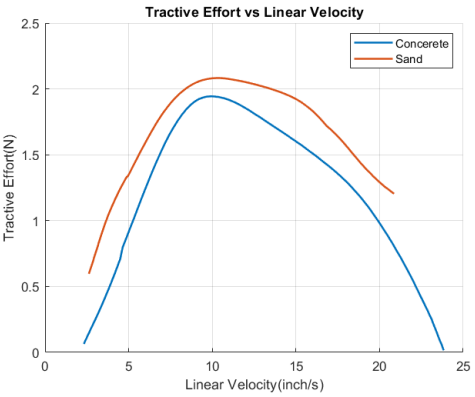

(b) Tractive Effort vs Linear Velocity

Fig. 13. Terrain comparison

$$TE = \frac{TG}{R} \tag{6}$$

In Figure 12(a),we observe the change in tractive effort concerning linear speed at various pressures on concrete surfaces. Figure12(b) demonstrates how power varies with linear speed under the same conditions. The data clearly shows that lower pressures correspond to higher tractive effort, resulting in increased power consumption. Conversely, higher pressures lead to lower tractive effort and consequently lower power consumption, indicating a direct correlation between tractive effort and power usage. Table I summarizes the maximum power and tractive effort for all pressures.

Furthermore, we conducted parallel experiments on compact sand (Figure 1(c)), as illustrated in Figure 13(a), which compares tractive effort and power at 3 PSI pressure. As anticipated, the power consumption on sand surpasses that on concrete, confirming our intuition through experimental validation.

Pressure (PSI)	Max P (W)	Max TE (N)
1	16.47	2.19
2	14.36	2.17
3	13.49	2.03
4	10.69	1.55
5	10.42	1.49

TABLE I
SUMMARY OF EXPERIMENTAL RESULT

B. Shell Variation

To understand how the thickness of the elastomer affects the dynamic behavior of the ball, the same study was conducted on two different shells with different thickness, one with 1/4' of thickness and other slightly higher. The figure 14 illustrates the comparison of Power and Tractive effort for two different shells at constant pressure of 3 PSI.

Figure 14 clearly shows that Shell-1, which has a thickness of 1/4', generates less tractive force and consumes less power compared to Shell-2, which has the thicker shell. This indicates that while the thicker shell provides more traction, but it also adds more weight to the ball. As a result, the effective radius of the pendulum is compromised, affecting the power consumption of the robot.

C. Water Test

Figure 15 showcases the power curve of the robot operating at 3 PSI in water. A comparison with the concrete and sand environments reveals starkly different behaviors of the robot in water. This discrepancy warrants further investigation to draw accurate analogies and comprehend the unique dynamics of the robot's performance in aquatic environments.

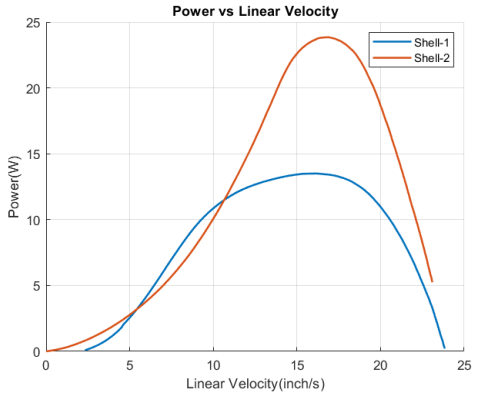

(a) Power vs Linear Velocity

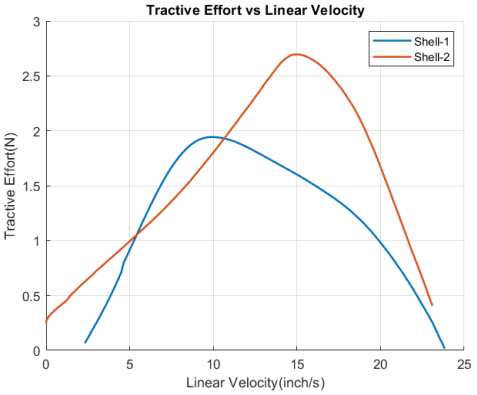

(b) Tractive Effort vs Linear Velocity

Fig. 14. Shell comparison

V. CONCLUSIONS

In summary, our study delves into the dynamic behavior of soft-shelled robotic systems, focusing on how terrain variation and shell thickness impact tractive effort and power consumption. Through rigorous experimentation and analysis, we've gained valuable insights into optimizing robot design and operation.

Our experiments across different terrain, like concrete and sand, revealed significant variations in tractive effort and power consumption. Lower pressures generally lead to higher tractive effort and power usage, while higher pressures result in the opposite. This direct relationship highlights the importance of managing these parameters for efficient robot performance across diverse terrains, and pressure control.

Furthermore, our exploration of shell variation highlighted the effects of elastomer thickness on tractive force and power consumption. We found that while thicker shells offer increased traction, they also add weight, compromising the pendulum's effective radius and impacting power consumption. This underscores the complex trade-offs inherent in shell design.

Overall, our research contributes insights for enhancing the performance and efficiency of soft-shelled robotic systems in real-world applications. By considering factors like terrain variation and shell thickness, designers can make informed decisions to optimize robot performance.

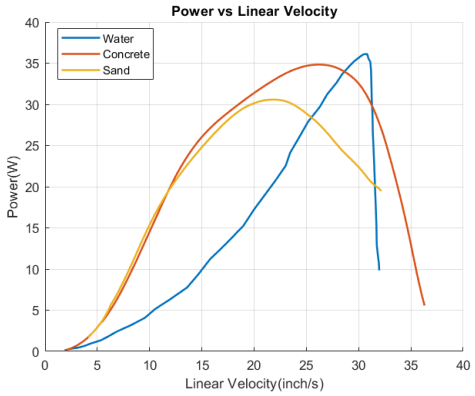

Fig. 15. Power vs Linear Velocity in water

This study further can be expanded to control the pressure inside the robot autonomously by identifying the terrain with the help of onboard sensors and systems.

VI. ACKNOWLEDGEMENT

The authors gratefully acknowledge the support provided by the Texas A&M Chancellor's Research Initiative and the Texas Governor's Research Initiative.

REFERENCES

[1] G. Heiken, D. Vaniman, and B. French pp. 85–91, 1991.
[2] R. Arvidson, P. D. Jr, J. Grotzinger, M. Heverly, J. Shechet, S. Moreland, M. Newby, N. Stein, A. Steffy, F. Zhou, A. Zastrow, A. Vasavada, A. Fraeman, and E. Stilly, "Relating geologic units and mobility system kinematics contributing to curiosity wheel damage at gale crater, mars," *Journal of Terramechanics*, vol. 73, pp. 73–93, 2017.
[3] M. Li, H. Sun, L. Ma, P. Gao, D. Huo, Z. Wang, and P. Sun, "Special spherical mobile robot for planetary surface exploration: A review," *International Journal of Advanced Robotic Systems*, vol. 20, no. 2, p. 17298806231162207, 2023.
[4] A. Behar, J. Matthews, F. Carsey, and J. Jones, "Nasa/jpl tumbleweed polar rover," in *2004 IEEE Aerospace Conference Proceedings (IEEE Cat. No.04TH8720)*, vol. 1, p. 395 Vol.1, 2004.
[5] Y. Liu, Y. Wang, X. Guan, Y. Wang, S. Jin, T. Hu, W. Ren, J. Hao, J. Zhang, and G. Li, "Multi-terrain velocity control of the spherical robot by online obtaining the uncertainties in the dynamics," *IEEE Robotics and Automation Letters*, vol. 7, no. 2, pp. 2732–2739, 2022.
[6] M. A. Arif, A. Zhu, H. Mao, X. Zhou, J. Song, Y. Tu, and P. Ma, "Design of an amphibious spherical robot driven by twin eccentric pendulums with flywheel-based inertial stabilization," *IEEE/ASME Transactions on Mechatronics*, pp. 1–13, 2023.
[7] T. J. Ylikorpi, A. J. Halme, and P. J. Forsman, "Dynamic modeling and obstacle-crossing capability of flexible pendulum-driven ball-shaped robots," *Robotics and Autonomous Systems*, vol. 87, pp. 269–280, 2017.
[8] M. Oevermann, D. Pravecek, G. Jibrail, R. Jangale, and R. Ambrose, "Roboball: An all-terrain spherical robot with a pressurized shell," in *2024 IEEE International Conference on Robotics and Automation (ICRA)*, 2024.
[9] M. Oevermann, M. P. Dravid, G. Jibrail, J. Janak, R. Jangale, D. McDougall, D. Dugas, and R. O. Ambrose, *A Soft Spherical Robot for Lunar Crater Exploration*.
[10] P. Patil and S. Yadav, "Analysis of gear box performance curves optimal selection of gear ratios," 05 2015.